Advances in Energy Science and Technology

Vol. 1, No. 4| Apr 2025

AEST

Exergoeconomic analysis of a geo-thermal power-plant with a comparative optimization using classical, meta-heuristic and reinforcement learning algorithms and sensitivity analysis with machine learning approach

Mahan Ahmadi Rahmatabadi [a], Mohammad Hossein Karim [a], S. Talebi [a, *], Mohsen Mardani [b], Seyed Hossein Hosseinian [c], Gevork B. Gharehpetian [c]

[a] *Department of Energy Engineering and Physics, Amirkabir University of Technology (Tehran Polytechnic), Tehran, Iran.*
[b] *ACECR, Amirkabir University of Technology Branch, Tehran, Iran.*
[c] *Department of Electrical Engineering, Amirkabir University of Technology (Tehran Polytechnic), Tehran, Iran.*

Keywords

Geo-Thermal Power Plant
Exergoeconomy
Machine Learning
Reinforcement Learning

Article Info

DOI: 10.22060/aest.2026.25579.1004

Received date: 6 January 2026

Accepted date 28 February 2026

Published date 1 April 2026

* **Corresponding author:**
Sa.talebi@aut.ac.ir

Abstract

Geothermal energy is a clean, and renewable source of energy with the ability to provide a continuous source of energy for electricity generation. In the current study, a detailed thermodynamic model of the geothermal power plant is developed and analyzed using the energy and exergy analysis methods in order to identify the major sources of irreversibility, efficiency reduction, and performance limitation within the geothermal power plant components. To improve the efficiency and performance of the geothermal power plant, a multi-objective optimization strategy using metaheuristic, classical, and reinforcement learning algorithms is implemented to maximize the net power and exergy efficiency, and the investment and operation costs are minimized. The results are useful for the optimal design and development of efficient and cost-effective geothermal power plants using the capabilities of the optimization algorithms to obtain an effective compromise between the thermodynamic and cost-based performance parameters.

Graphical Abstract

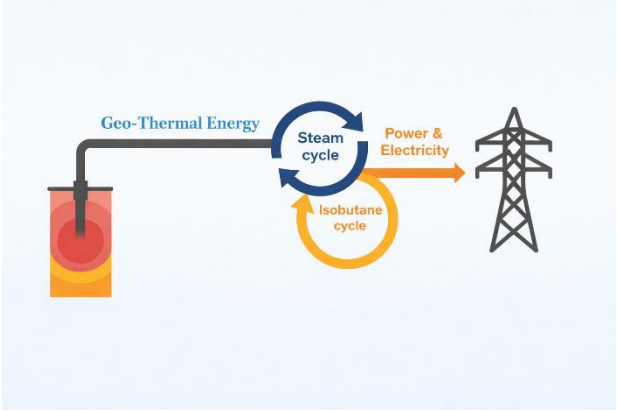

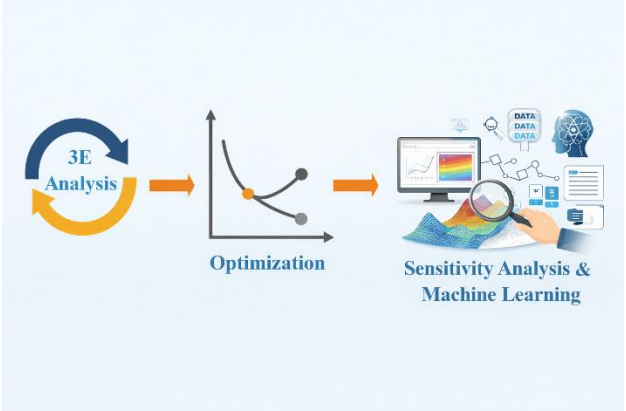

1. Introduction

Geothermal energy represents one of the few renewable energy resources capable of delivering both baseload electricity and direct thermal energy with relatively limited environmental disturbance. As global energy systems continue to shift toward lower carbon intensity, geothermal resources are increasingly viewed as stable contributors that can complement intermittent renewable technologies. Despite these advantages, the practical deployment and long-term economic competitiveness of geothermal systems remain closely tied to detailed thermodynamic and financial performance assessments. In this regard, exergy analysis has emerged as a particularly informative approach. Unlike conventional energy analysis, which focuses primarily on energy quantity, exergy analysis evaluates energy quality and tracks the mechanisms responsible for irreversible losses within system components. By applying the second law of thermodynamics, this method provides insight into the true sources of performance degradation and helps identify opportunities for system-level improvement. When economic considerations are incorporated through exergoeconomic analysis, thermodynamic inefficiencies can be directly associated with cost generation mechanisms, thereby offering valuable guidance for system design and operational optimization [1].

Efforts to improve geothermal system efficiency have increasingly relied on the integration of optimization techniques within thermo-economic assessment frameworks. Several studies have explored this direction across different geothermal plant configurations. Yilmaz [2], for instance, investigated the thermo-economic optimization of a hybrid system integrating a flash-binary geothermal power plant with an alkaline water electrolysis unit for hydrogen production. Through the implementation of a genetic algorithm (GA), the study demonstrated measurable reductions in the unit production costs of both electricity and hydrogen, illustrating the potential of geothermal resources as drivers of clean fuel production. The analysis further revealed that major system components, including the electrolysis unit, turbine stages, and heat exchange equipment, accounted for a significant portion of total exergetic cost formation. Earlier research had already established a technological foundation for geothermal-assisted hydrogen production. Jónsson et al. [3] examined the feasibility of utilizing geothermal heat in high-temperature steam electrolysis applications, providing early evidence of the technical viability of such systems. Building on this work, Sigurvinsson et al. [4, 5] evaluated both the operational performance and techno-economic characteristics of high-temperature electrolysis (HTE) processes coupled with geothermal heat sources. Kanoglu and his team [6, 7] went a step further by diving into detailed exergoeconomic studies of geothermal-supported high-temperature electrolysis and hydrogen liquefaction systems. These studies show just how valuable thermo-economic methods are becoming for understanding both the performance and sustainability of geothermal energy technologies.

Despite these advances, there are still gaps in the research. A closer look at the existing studies, including Yilmaz's work [2], shows that most efforts have focused on applying individual optimization methods to specific integrated systems. Broader questions about how geothermal energy can be more widely and efficiently integrated remain largely unexplored. Comparative analyses involving multiple optimization paradigms remain relatively limited, particularly for studies centered on the core geothermal power generation cycle itself. Furthermore, systematic evaluations comparing classical optimization approaches, metaheuristic algorithms, reinforcement learning methods, and emerging data-driven optimization techniques are still uncommon within geothermal system research. The application of machine learning methods to perform advanced sensitivity analyses and to derive empirical performance relationships has also received relatively little attention. Many existing optimization studies concentrate on a restricted number of algorithmic techniques or prioritize single-output system objectives,

such as hydrogen production, without fully addressing how different optimization strategies interact with the highly nonlinear design characteristics of combined flash-organic Rankine cycle (ORC) geothermal power plants.

In this research, we comprehensively assess and optimize a flash-binary geothermal power plant equipped with both steam and ORC subsystems. This study focuses on four key goals. First, detailed energy, exergy, and exergoeconomic analyses are performed to identify the principal sources of thermodynamic irreversibility and cost-related inefficiencies throughout the system. Second, a broad spectrum of optimization techniques is implemented and comparatively evaluated. These include classical optimization methods such as Simplex, GLPK, Gurobi, IPOPT, and Couenne, as well as metaheuristic approaches including Genetic Algorithm, Particle Swarm Optimization, Grey Wolf Optimizer, and NSGA-II, in addition to a reinforcement learning-based optimization framework. Third, a comprehensive sensitivity analysis is conducted and enhanced through machine learning models to establish reliable polynomial correlations between key operational variables and overall system performance indicators. Finally, the thermodynamic models developed in this study are validated using multiple simulation environments, namely EES, ASPEN Plus, and Python-CoolProp, to ensure consistency and reliability of the simulation results. The final goal is to determine optimization strategies that can simultaneously enhance energy and exergy efficiencies, increase net power generation, and reduce total product cost, thereby contributing to the development of more efficient and economically competitive geothermal power systems.

2. Thermodynamic Model

This section provides a description of the proposed model for generating electricity using geothermal energy. The model consists of a combined cycle integrating a steam turbine and an Organic Rankine Cycle (ORC). The working principle of the system is shown in **Fig. 1**. The system utilizes a liquid-dominated geothermal resource with a reservoir temperature of 200°C. The geothermal water enters the plant at 159°C and 600 *kPa* with a total mass flow rate of 100 *kg/s*. Within the cycle, the fluid is separated; the steam portion drives a steam turbine to produce electricity, while the remaining liquid water provides the heat input for the ORC unit. In the ORC, the geothermal liquid heats and vaporizes the organic working fluid, isobutane, in a primary heat exchanger. The superheated isobutane vapor then expands through an isobutane turbine to produce additional electrical power. The isobutane turbine exhaust is subsequently condensed in an air-cooled condenser and pumped back to the heat exchanger, completing the closed ORC loop.

The geothermal plant operates in a closed loop, preventing any emissions to the environment. After the geothermal water has given up its heat, it is entirely reinjected back into the underground reservoir through the injection well. The total power output from both the steam and isobutane turbines is supplied to the power grid. Approximately 20% of the ORC's output and 5% of the steam cycle's output are allocated for internal demands, such as powering pumps and condenser fans, values which align with those of existing geothermal plants. The analysis of the system is grounded in the principles of thermodynamics. The first law deals with the conservation of energy, while the second law, concerned with energy quality, entropy generation, and lost work potential, provides a powerful framework for optimizing the performance of the overall system. For the thermodynamic analysis and validation, Engineering Equation Solver (EES) and ASPEN Plus were used to simulate the cycle and calculate thermodynamic properties at all state points, with results validated against reference studies [2, 8]. For the optimization process, Python with the CoolProp library was employed to implement various algorithms and determine the system's optimal performance parameters.

Advances in Energy Science and Technology
Vol. 1, No. 4| Apr 2025
AEST

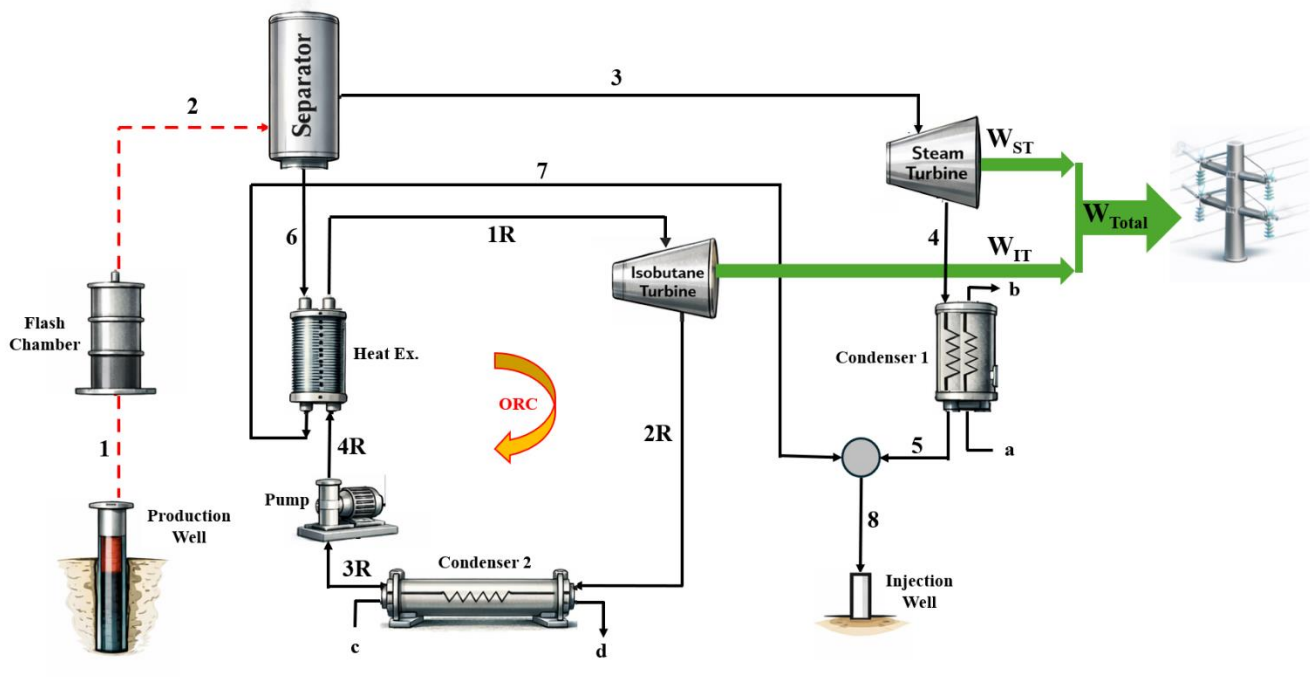

Fig. 1. Schematic diagram of electricity generation from geothermal energy using a combined steam turbine and isobutane (ORC) turbine system.

2.1 Energy Analysis

The system's energy analysis is carried out using the principles of mass and energy conservation. Each component is treated as an individual control volume, and for any control volume with an inlet i and an outlet o, the mass and energy balances can be written as follows:

$$\sum \dot{m}_i = \sum \dot{m}_o \tag{1}$$

$$\sum \dot{Q} - \sum \dot{W} = \sum \dot{m}_o h_o - \sum \dot{m}_i h_i \tag{2}$$

The following assumptions are adopted in the energy analysis:

- The system operates under steady-state conditions, and pressure drops in pipes, condenser, separator, and heat exchangers are neglected.
- The flow through the valve is assumed to be isentropic.
- The processes occurring in turbines and pumps are non-isentropic; therefore, isentropic efficiencies are introduced in the mathematical model to account for irreversibilities.
- The working fluid at the condenser outlet and evaporator outlet is assumed to be saturated liquid and saturated vapor, respectively.
- Changes in kinetics and potential energies are neglected.

The mass and energy balance equations corresponding to the individual components of the system are summarized in **Table 1**.

Table 1. Mass and energy balance equations for different components of the system.

Component	Equilibrium Equations	Component	Equilibrium Equations
Separator	$m_2h_2 = m_6h_6+m_3h_3$ $m_2 = m_6+m_3$	**Pump**	$W_{Pump} = m_{3R}(h_{4R}-h_{3R})$ $m_{3R} = m_{4R}$
Steam Turbine	$W_{ST} = m_3(h_3-h_4)$ $m_3 = m_4$	**Isobutane Turbine**	$W_{IT} = m_{1R}(h_{1R}-h_{2R})$ $m_{1R} = m_{2R}$
Condenser 1	$m_4(h_4-h_5) = m_a(h_b-h_a)$ $m_4 = m_5$ $m_a = m_b$	**Condenser 2**	$m_{3R}(h_{3R}-h_{4R}) = m_d(h_d-h_c)$ $m_{3R} = m_{4R}$ $m_c = m_d$
Heat Ex.	$m_6(h_6-h_7) = m_{1R}(h_{1R}-h_{4R})$ $m_6 = m_7$ $m_{1R} = m_{4R}$		

2.2 Exergy Analysis

Exergy represents the maximum useful work that can be extracted from a given form of energy. Exergy efficiency is a valuable indicator for evaluating both the energy quality and the performance of a thermodynamic system [9]. The exergy balance equations for each control volume, derived from the first and second laws of thermodynamics, are expressed as follow:

$$\dot{E}_Q + \sum_i \dot{m}_i e_i = \sum_o \dot{m}_o e_o + \dot{E}_W + \dot{E}_D \quad (3)$$

$$\dot{E}_Q = \left(1 - \frac{T_0}{T}\right)\dot{Q} \quad (4)$$

$$\dot{E}_W = \dot{W} \quad (5)$$

The following assumptions are adopted in the exergy analysis of the system:

- Only physical exergy of the flow streams is considered.
- Kinetic and potential exergy components are neglected due to negligible changes in velocity and elevation.
- Chemical exergy effects are ignored.

In this study, system performance is assessed through exergy analysis. The governing parameters include the exergy associated with work ($\dot{E}_W$) and heat transfer ($\dot{E}_Q$), alongside the rate of exergy destruction ($\dot{E}_D$). The terms i and o correspond to input and output streams. **Table 2** details the calculated fuel exergy, product exergy, and destruction exergy rates for each system component. According to Eq. (6), the fuel exergy is equal to the sum of the product exergy and the exergy destruction.

$$Ex_f = Ex_P + Ex_D \quad (6)$$

Table 2. Destruction exergy, fuel exergy, and product exergy rates for each component.

Component	Equilibrium Equations	Component	Equilibrium Equations
Separator	$Ex_f = Ex_2$ $Ex_p = Ex_2 + Ex_6$	**Pump**	$Ex_f = Ex_{3R} - Ex_{4R}$ $Ex_p = W_{Pump}$
Steam Turbine	$Ex_f = Ex_3 - Ex_4$ $Ex_p = W_{ST}$	**Isobutane Turbine**	$Ex_f = Ex_{1R} - Ex_{2R}$ $Ex_p = W_{IT}$
Condenser 1	$Ex_f = Ex_4 - Ex_5$ $Ex_p = Ex_b - Ex_a$	**Condenser 2**	$Ex_f = Ex_{3R} - Ex_{4R}$ $Ex_p = Ex_d - Ex_c$
Heat Ex. 1	$Ex_f = Ex_6 - Ex_7$ $Ex_p = Ex_{1R} - Ex_{4R}$		

2.3 Exergoeconomic Analysis

One of the most critical and fundamental analyses in the evaluation of power plants and systems is exergoeconomic analysis, also known as exergoeconomy. Exergoeconomy is an integrated analytical framework that combines concepts of exergy and economics to optimize energy systems. In this method, economic costs are directly linked to the exergetic efficiency of systems to identify points of energy waste and economic inefficiency. The primary objective is to achieve an optimal balance between thermodynamic performance and cost-effectiveness, leading to the design of more sustainable systems, such as power plants, heat recovery units, or heating and cooling systems. By assigning economic costs to exergy streams, engineers can make more informed decisions to reduce resource waste and improve overall system efficiency. According to Eqs. (7) and (8), the cost balance states that the sum of the costs associated with the output exergy streams of a fluid equals the sum of the costs of the input exergy streams plus the investment and operation and maintenance (O&M) costs.

$$\sum_e \dot{C}_{e,k} + \dot{C}_{W,k} = \sum_i \dot{C}_{i,k} + \dot{Z}_K^{Cl} + \dot{Z}_K^{OM} \quad (7)$$

$$\dot{Z}_K = \dot{Z}_K^{Cl} + \dot{Z}_K^{OM} = Z_K^{Cl} \times CRF \times \varphi / t \quad (8)$$

$$\dot{C}_i = c_i \dot{E}X_i \quad (9)$$

The values of the key economic parameters including: capital recovery factor (CRF), maintenance factor (φ), annual operating hours (t), interest rate (i), and useful life (N), used in Eqs. (7) and (8) are provided in **Table 3**. Furthermore, **Table 4** presents the detailed exergoeconomic calculations for the various system components. Also purchased cost and cost rates of each component are presented in **Table 5** according to [2].

Advances in Energy Science and Technology
Vol. 1, No. 4| Apr 2025
AEST

Table 3. Economic Parameters.

Variable	Description	Value
CRF	Capital Recover Factor	$\frac{i(1+i)^N}{(1+i)^N-1}$
φ	maintenance factor	1.06
t	hours per year	7446
i	discount rate	10%
N	system life	20 Year

Table 4. Exergoeconomic Calculations.

Component	Cost rate balance	Auxiliary Equation
Flash Chamber	$C_1 + \dot{Z_{F,ch}} = C_2$	-
Steam Turbine	$C_3 + \dot{Z_{ST}} = C_{W,ST} + C_4$ $\frac{C_3}{Ex_3} = \frac{C_4}{Ex_4}$	$\frac{C_3}{Ex_3} = \frac{C_4}{Ex_4}$
Condenser 1	$C_a - C_b + \dot{Z_{cond1}} = C_4 - C_5$	$\frac{C_4}{Ex_4} = \frac{C_5}{Ex_5}$
Heat Ex.	$C_6 - C_7 + \dot{Z_{HE1}} = C_{1R} - C_{4R}$	$\frac{C_6}{Ex_6} = \frac{C_7}{Ex_7}$
Isobutane Turbine	$C_{1R} + \dot{Z_{IT}} = C_{W,IT} + C_{2R}$	$\frac{C_{1R}}{Ex_{1R}} = \frac{C_{2R}}{Ex_{2R}}$
Condenser 2	$C_d - C_c + \dot{Z_{cond2}} = C_{3R} - C_{4R}$	$\frac{C_{2R}}{Ex_{2R}} = \frac{C_{3R}}{Ex_{3R}}$
Pump	$C_3 + C_{W,pump} + \dot{Z_{pump}} = C_{4R}$	$\frac{C_{3R}}{Ex_{3R}} = \frac{C_{4R}}{Ex_{4R}}$

Table 5. Purchased cost and cost rates of each component.

Component	C_k (10^3 \$)	$\dot{Z_k}^{CL}$ (\$/h)	$\dot{Z_k}^{OM}$ (\$/h)	$\dot{Z}_k$ (\$/h)
Flash Chamber (FC)	20.500	0.5295	0.1039	0.6333
Separator	65.200	1.684	0.3303	2.014
Steam Turbine (ST)	942.600	24.350	4.775	29.12
cooled condenser (Water)	242.900	6.274	1.231	7.504
Heat Exchanger	465.600	9.004	1.766	10.77
Isobutane Turbine (IT)	973.400	25.14	4.931	30.07
Cooled Condenser (Air)	229.900	5.938	1.165	7.103
Pump	153.400	3.962	0.7772	4.739

3. Optimization

Optimization of engineering systems is necessary to achieve maximum performance, optimal cost, and sustainability [10]. In renewable energy systems, optimization algorithms provide a systematic and organized way of searching the decision

space while satisfying the system constraints. The objective function for optimizing this system is given in Eq. (10), and the constraints on this system are given in **Table 6**.

The optimization algorithms want to maximize the composite objective function (F) defined in Eq. (10), which is a weighted sum of the system's exergetic efficiency (η_{ex}) and the complement of its total cost rate ($C_{P,total}$). The decision variables for this maximization are the isobutane turbine inlet temperature (T_{1R}), Condenser1 outlet pressure (P2), and the isentropic efficiencies of the steam turbine, isobutane turbine, and pump ($\eta_{iso-ST}, \eta_{iso-IT}, \eta_{iso-\text{pump}}$). The weighting factors W_{eff} and W_{cost}, bounded between 0 and 1 as per Eq. (11) and summing to unity per Eq. (12), determine the relative priority assigned to thermodynamic performance versus economic cost in the final solution. In the optimization process of this study, the weighting factors W_{eff} and W_{cost} are set to 0.88 and 0.12, respectively [8]. The selection of these values depends on the priorities of the designer and represents the relative importance of each objective function. The search for the optimal decision variables is constrained within the physically realistic bounds, ensuring the search for the optimal decision variables is within the technically realistic bounds for the temperatures, pressures, and efficiencies of the components involved.

$$Max\ F\left(T_{1r}.P_5.\eta_{iso-ST}.\eta_{iso-IT}.\eta_{iso-pump}\right) = W_{eff} \times \eta_{ex} + W_{cost} \times \left(1 - C_{P,total}\right) \quad (10)$$

$$0 \leq W_{eff}.W_{cost} \leq 1 \quad (11)$$

$$W_{eff} + W_{cost} = 1 \quad (12)$$

Table 6. Optimization constraints.

No.	Variable	Description	Feasible Range
1	T_{1R}	Isobutane turbine input temperature	$130 \leq T_{1R}(C) \leq 150$
2	P_5	Condenser1 outlet pressure	$5 \leq P_5(kPa) \leq 15$
3	η_{iso-ST}	Steam turbine isentropic efficiency	$70 \leq \eta_{iso-ST}\ (\%) \leq 90$
4	η_{iso-IT}	Isobutane turbine isentropic efficiency	$70 \leq \eta_{iso-\text{IT}}\ (\%) \leq 90$
5	$\eta_{iso-pump}$	Pump isentropic efficiency	$70 \leq \eta_{iso-\text{pump}}\ (\%) \leq 90$

Different optimization algorithms are applied in this system to optimize the system with different approaches; these algorithms are explained as follow:

Classic optimization algorithms, form the theoretical foundation of the field and provide mathematically robust solutions for problems with well-defined and convex structures. The Simplex method is a fundamental algorithm for solving linear programming models, efficiently moving along the feasible region's vertices to locate the optimal solution [11]. Open-source solvers such as GLPK address linear and mixed-integer problems using simplex, interior-point, and branch-and-cut techniques, providing a reliable deterministic reference [12]. Advanced solvers like Gurobi handle linear programming, mixed integer programming, and quadratic programming formulations with high precision [13], while IPOPT is particularly suited for large-scale nonlinear programs involving thermodynamic complexities [14]. For non-convex and discrete formulations, Couenne serves as a capable global solver for mixed-integer nonlinear optimization [15]. Together, these classical methods establish dependable baselines and ensure accuracy for structured optimization problems.

On the other hand, metaheuristic or nature-inspired algorithms are intended for solving complex, nonlinear, and/or non-convex optimization problems for which traditional optimization methods might be inefficient or diverge from the solution set. The Genetic Algorithm (GA) mimics the process of natural selection and evolution by implementing selection, crossover, and mutation operators for efficient search in large and multimodal solution spaces [16]. The Particle Swarm Optimization (PSO) is based on the social behavior of bird flocks, where each particle is influenced by its individual and social best positions [17]. The Non-Dominated Sorting Genetic Algorithm II (NSGA-II) is one of the most prominent optimization algorithms for solving multi-objective optimization problems, which is capable of achieving Pareto optimal sets [18]. The Grey Wolf Optimizer (GWO) is motivated by the social hierarchy and hunting behavior of the grey wolf species and has demonstrated promising exploration capacity with ease of implementation [19]. These optimization algorithms are highly useful for designing renewable energy systems, which are characterized by nonlinear, uncertain, and/or highly coupled relationships.

Recently, a new data-driven optimization technique based on Reinforcement Learning (RL) optimization has gained popularity. In this technique, an intelligent agent continually interacts with its environment and receives feedback in the form of rewards, learning a policy to optimize cumulative rewards. Unlike other techniques that follow a fixed mathematical formulation, RL techniques can adapt to changing conditions and uncertainties in a system, making them suitable for sequential and time-dependent optimization, such as in energy optimization and control [20]. The recent studies have provided a significant amount of evidence of the potential of RL optimization in solving various industrial and combinatorial optimization problems through adaptive learning, robustness, and decision-making.

4. Sensitivity analysis with machine learning approach

In this study, a sensitivity analysis was conducted to further evaluate the system's behavior. This analysis examined the overall exergy efficiency of the system under variations in the inlet temperature and pressure of both the isobutane and steam turbines, and the results are presented in Results section. To obtain a more comprehensive assessment, the governing equations for the sensitivity analysis were derived using machine learning techniques. Machine learning allows computers to automatically discover patterns, correlations, and structures in data, enabling them to make predictions or decisions without being explicitly programmed [21]. Such data-driven models give better insights into the performance of the system, aid in the identification of critical operational dependencies, and hence contribute to the optimization process. Polynomial regression was employed to fit the nonlinear relationships between input parameters and efficiency, providing a continuous, differentiable model for rapid sensitivity analysis and optimization guidance. Polynomial regression is a flexible machine learning algorithm that models non-linear relationships by transforming input features into polynomial terms, making it particularly effective for capturing complex patterns in data across scientific and engineering disciplines [22].

To evaluate the accuracy and reliability of the developed machine learning models, statistical performance metrics such as the coefficient of determination (R^2-score), Eq. (13) and the mean squared error (MSE), Eq. (14) were employed. The R^2-score measures the proportion of variance in the predicted output that is explained by the input variables, providing an indication of how well the model captures the underlying relationship between system parameters and performance indicators [23]. In contrast, the MSE quantifies the average squared difference between predicted and actual values, reflecting the

magnitude of prediction errors and the overall robustness of the model [23]. Together, these metrics offer a comprehensive assessment of model performance, ensuring that the machine learning-based sensitivity analysis yields accurate, consistent, and reliable predictions for evaluating and optimizing the geothermal power system.

$$R^2 = 1 - \frac{\sum_{i=1}^{n}(y_i - \hat{y}_i)^2}{\sum_{i=1}^{n}(y_i - \bar{y}_i)^2} \quad (13)$$

$$MSE = \frac{1}{n}\sum_{i=1}^{n}(y_i - \hat{y}_i)^2 \quad (14)$$

5. Results

After modelling the geo-thermal power plant system via EES, Aspen and Python, the calculated temperature, pressure, enthalpy, entropy of each state is presented in **Table 7** and the results are validated with the results of paper in ref. [8]. The results show very little difference between each software approaches and reference; this shows the results are reliable and reproducible.

Table 7. Temperature, pressure, enthalpy (h) and entropy (s) of each state.

State	Temperature (C)			Pressure *(kPa)*			h *(kJ/kg)*				s *(kg/kg.K)*			
	Reference	EES	ASPEN	Reference	EES	ASPEN	Reference	EES	ASPEN	CoolProp	Reference	EES	ASPEN	CoolProp
0	25	25	25	100	100	101.3	104.9	104.8	104.8	104.91	0.3672	0.3669	0.367	0.367
1	200	200	200	1555	1555	1555	853.3	852.4	852.3	852.27	2.331	2.331	2.331	2.33
2	158.8	200	158.8	600	1555	600	852.3	852.6	852.3	852.27	2.352	2.331	2.353	2.33
3	158.8	158.9	158.8	600	600	600	2756	2793	2752	2756.11	6.759	6.431	6.759	6.759
4	45.81	45.82	45.83	10	10	10	2233	2149	2232	2233.02	7.049	6.787	7.050	7.048
5	45.81	45.82	45.83	10	10	10	191.8	191.8	192.3	191.80	0.6492	0.6493	0.6494	0.649
6	158.8	158.9	158.8	600	600	600	670.4	670.7	662.3	670.26	1.931	1.932	1.931	1.930
7	76	76	76	600	600	600	318.1	318.6	312.3	318.67	1.027	1.027	1.027	1.027
1R	148.8	150	147.9	2100	2100	2100	802.7	805.7	802.7	801.81	2.689	2.696	2.946	2.685
2R	100.41	101.7	100.4	400	400	400	732.5	735.1	730.7	731.55	2.722	2.729	2.977	2.719
3R	29.61	29.61	29.61	400	400	400	270.4	270.8	270.7	270.18	1.243	1.245	1.502	1.242
4R	30.59	30.75	31.02	2100	2100	2100	274.1	274.5	273.7	273.07	1.245	1.246	1.361	1.241

The performance of various optimization algorithms, including Genetic Algorithm, Particle Swarm Optimization, Grey Wolf Optimizer, NSGA-II, Reinforcement Learning, and several deterministic solvers (Simplex, GLPK, Gurobi, IPOPT,

Couenne), was evaluated against the BASE case design. The comparative results for key performance metrics are summarized in **Table 8**.

The BASE case operation results in a total cost rate ($C_{P,total}$) of 6432.905 *$/h* and an exergy efficiency of 29.54%. Among the algorithms, the stochastic optimizers significantly outperformed the deterministic solvers, with the latter converging to the BASE case values. This indicates the complexity and non-convex nature of the optimization landscape.

Notably, the NSGA-II algorithm demonstrated the best overall performance, achieving the highest net power output (W_{net}) of 83.98 *kW* and the highest exergy efficiency of 30.38%. While NSGA-II yielded a slightly lower isentropic efficiency for the steam turbine (η_{iso-ST}) compared to some algorithms, it achieved the highest isentropic efficiency for the isobutane turbine (η_{iso-ST}) at 89.22%, effectively maximizing power production from the cycle. Most strikingly, NSGA-II achieved a dramatic reduction in the total cost rate, lowering it to just 387.38 *$/h*. This represents a reduction of over 90% compared to the BASE case, demonstrating an exceptional balance between the dual objectives of maximizing exergy efficiency while simultaneously minimizing total product cost.

Other algorithms like GA and GWO also provided competitive results, with exergy efficiencies of 30.36% and 30.31%, and cost rates of 5617.57 *$/h* and 6103.09 *$/h*, respectively. The RL algorithm, while achieving a relatively low-cost rate of 4622.41 $/h, resulted in a lower exergy efficiency of 28.49% and net power output of 78.75 *kW*, indicating a bias towards cost reduction.

Due to its superior capability in handling the multi-objective nature of the problem, the Pareto front obtained from the NSGA-II optimization is presented in **Fig. 2.** This front clearly illustrates the trade-off between the two conflicting objectives, showcasing a set of optimal solutions from which the most balanced configuration was selected for final comparison.

System energy and exergy efficiencies are calculated via the ratio of output to input energy and exergy, respectively, and the total generated electricity of the system is calculated as follow:

$$W_{net} = 0.95 * W_{st} + 0.80 * W_{IT} - W_{Pump} \quad (15)$$

In Eq. (15), 5% and 10% of the generated electricity is considered as the loss of the steam and isobutane turbines, respectively. The Pareto front obtained from the NSGA-II optimization, illustrating the trade-off between the two conflicting objectives, is presented in **Fig. 2**. Each blue circle represents a solution, where any improvement in one objective would lead to deterioration in the other.

A sensitivity analysis on the weight factors was performed to investigate the impact of each objective on the optimal solution. Based on this analysis, three extreme points on the Pareto front are highlighted. The yellow star corresponds to the solution for which only efficiency is taken into account, resulting in the highest exergy efficiency of 33.46% but with a relatively high total cost. On the other hand, the black square corresponds to the minimum cost solution, resulting in the lowest total cost of 387.37 *$/h* with an exergy efficiency of 30.38%. The red diamond corresponds to the solution for which equal importance is assigned to both objectives, achieving an efficiency of 33.46% at a moderate cost.

Table 8. Optimization results of different optimization algorithms.

	BASE	GA	PSO	GWO	NSGA-II	RL	Simplex	GLPK	Gurobi	IPOPT	Couenne
P5 (KPa)	10	5.0395	13.2665	12.7483	13.8589	5	10	10	10	10	10
T1R (C)	140.00	131.6738	135.3528	140.4214	148.173	130	140	140	140	140	140
Eta_ST (%)	80.0	77.84	80.68	80.89	75.87	83.30	80.0	80.0	80.0	80.0	80.0
Eta_IB (%)	80.0	86.51	80.99	83.51	89.22	70.0	80.0	80.0	80.0	80.0	80.0
Eta_Pump (%)	80.0	82.02	84.09	85.77	73.65	70.0	80.0	80.0	80.0	80.0	80.0
Eta_Energy (%)	10.9263	11.23	11.04	11.21	11.24	10.54	10.93	10.93	10.93	10.93	10.93
Eta_Exergy (%)	29.5415	30.36	29.86	30.31	30.38	28.49	29.54	29.54	29.54	29.54	29.54
W_Steam (kW)	42.9588	41.7981	43.3222	43.4391	40.7395	44.7480	42.9588	42.9588	42.9588	42.9588	42.9588
W_IsoButane (kW)	40.4059	43.9622	41.0575	42.1819	44.7481	35.5791	40.4059	40.4059	40.4059	40.4059	40.4059
W_Pump (kW)	1.7070	1.8277	1.8380	1.8270	1.5087	1.5726	1.7070	1.7070	1.7070	1.7070	1.7070
W_net (kW)	81.6577	83.9326	82.5416	83.7941	83.9788	78.7545	81.6577	81.6577	81.6577	81.6577	81.6577
$C_{P,total}$ ($/h)	6432.905	5617.566	5782.773	6103.091	387.375	4622.405	6432.905	6432.905	6432.905	6432.905	6432.905

Based on a careful trade-off analysis, the optimal point that is highlighted by the red star was selected with a higher priority on efficiency (W_{eff}=0.88) while still maintaining a low total cost (W_{cost}=0.12). This configuration achieves an exergy efficiency of 30.38% and a remarkably low total cost of 387.37 *$/h*. Although this point indicates a slight decrease in efficiency compared to the maximum efficiency solution, it provides a tremendous cost reduction of over 90%. This well-balanced solution successfully identifies the key objective of the optimization process, which is to attain maximum efficiency with minimal economic cost.

Advances in Energy Science and Technology
Vol. 1, No. 4| Apr 2025
AEST

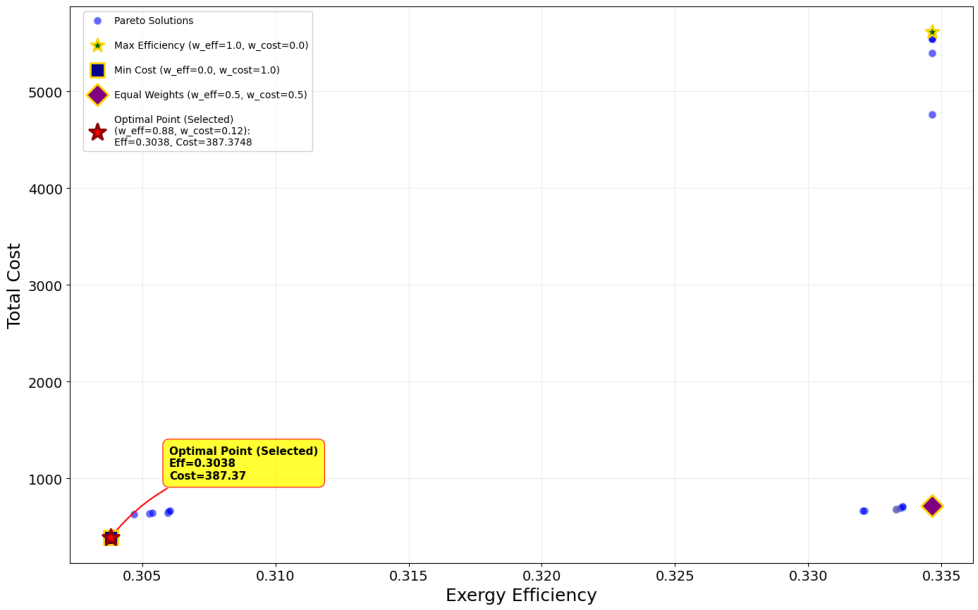

Fig. 2. Pareto front: Effect of different weights on the optimal solutions.

Fig. 3 presents the sensitivity analysis of the system's exergy efficiency under variations in the inlet conditions of the isobutane and steam turbines. Sub-figures (a), (b), (c), and (d) illustrate the influence of inlet temperature and pressure on exergy efficiency. As shown in **Fig. 3a**, increasing the isobutane turbine inlet temperature leads to a slight but continuous decrease in exergy efficiency, indicating enhanced irreversibilities at higher temperatures. In contrast, Figure 3b demonstrates that increasing the isobutane turbine inlet pressure improves exergy efficiency, although the rate of improvement gradually diminishes at higher pressures. **Fig. 3c** and **3d** reveal that increasing both the inlet temperature and pressure of the steam turbine results in a monotonic increase in exergy efficiency. This behavior suggests that higher-quality steam at elevated temperature and pressure enhances the useful work potential of the cycle and reduces relative exergy destruction.

The sensitivity analysis is conducted using a polynomial regression–based machine-learning approach, generating accurate second- and third-order correlations for each operating parameter. The high values of R^2 (approximately 99.9%) and the low values of MSE confirm the robustness and predictability of the developed models. The correlations offer a fast and reliable alternative to simulations, allowing for efficient performance prediction and optimization of the system.

y = - 0.634956893323+ 0.00653704127086*x- 0.00001509925852*x^2 + 0.00000001144228*x^3

y = 0.134793890976 +0.00000011389334*- 0.00000000000002*x^ 2

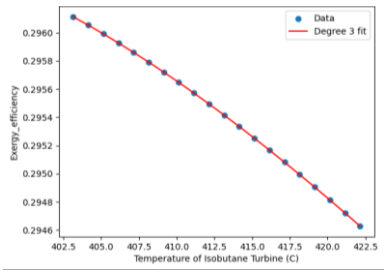

(a)

R^2 (%): 99.9999 %

MSE (%): 8.2582e-06 %

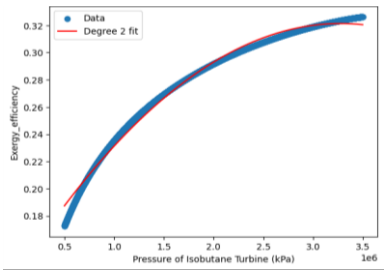

(b)

R^2 (%): 99.2287 %

MSE (%): 0.28695 %

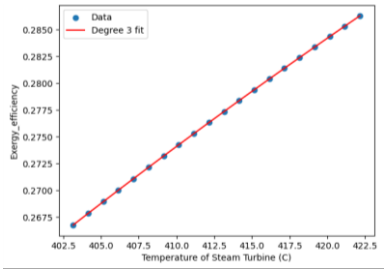

(c)

y = -1.4533431321 + 0.0090779842*x - 0.0000160029*x^2 + 0.0000000101*x^3

R^2 (%): 99.9999 %

MSE (%): 1.7702e-06 %

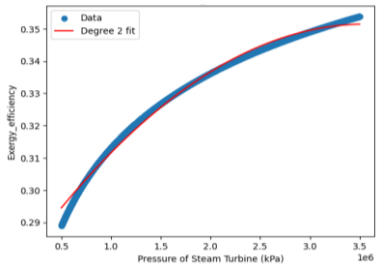

(d)

Y = 0.274374939476+ 0.00000004331922*x- 0.00000000000001*x^ 2

R^2 (%): 99.3721 %

MSE (%): 0.1097 %

Fig. 3. Sensitivity analysis of steam and isobutane turbines with ML approach.

6. Discussion and future works

In continuation of the present work, several directions are suggested for future research. First, incorporating additional components such as a recuperator is recommended to further improve the system's energy and exergy efficiencies. Previous research studies have shown that the incorporation of a recuperator in geothermal power plant cycles can lead to improved power and system efficiency [24]. Secondly, the system should be assessed and compared with other forms of renewable sources of energy, such as solar and wind power. This will provide further insight into the advantages and disadvantages of the geothermal system under different environmental conditions. Finally, future research is recommended on assessing the ability of the proposed system to be used as a combined system that can be used to generate other forms of energy, such as hydrogen, heat, and cooling. Hybrid configurations that simultaneously support power generation and hydrogen or thermal/cooling co-production could offer substantial improvements in overall efficiency, flexibility, and sustainability [25].

7. Conclusion

In this research, a green power generation system by geothermal energy with the aim of energy, exergy and exergoeconomic analysis is modeled, analyzed, and optimized through EES, ASPEN and Python. Five primary parameters affecting system performance, namely, the inlet temperature of the isobutane turbine, outlet pressure of the first condenser, and the isentropic efficiencies of the steam turbine, isobutane turbine, and pump are defined as decision variables and their individual and combined impacts on the overall system output are comprehensively investigated. To improve the system's performance, a range of optimization algorithms, including classical, metaheuristic, and reinforcement learning-based methods, are employed. The results reveal that the NSGA-II algorithm was the best algorithm in improving the system's thermodynamic performance and lowering economic costs, achieving maximum energy and exergy efficiencies of 11.24% and 30.38%, respectively and lowest total cost of 387.375 *$/h*.

Author contributions

M.A.R.: Writing – original draft, Visualization, Project administration, Investigation, Python programming & simulation, Modeling, Optimization Algorithms, Machine Learning, Writing – review & editing. **M.H.K.:** Writing, Modeling, EES Programming, Visualization. **S.T.:** Writing – review & editing, Validation, Methodology, Supervision. **M.M.**: Writing – review & editing, Validation, Methodology, Supervision. **Seyed Hossein Hosseinian:** Writing – review & editing, Validation**. G. B. G.:** Writing – review & editing, Validation.

Declaration of competing interest

The authors declare that they have no known competing financial interests or personal relationships that could have appeared to influence the work reported in this paper.

Data availability

No data is used in this article.

References

[1] A. Bejan, G. Tsatsaronis, Thermal Design and Optimization, John Wiley & Sons, 1996.

[2] C. Yilmaz, Thermoeconomic modeling and optimization of a hydrogen production system using geothermal energy, Geothermics 65 (2017) 32–43.

[3] V.K. Jónsson, R.I. Gunnarsson, B. Árnason, T.I. Sigfússon, The feasibility of using geothermal energy in hydrogen production, Geothermics 21 (1992) 673–681.

[4] J. Sigurvinsson, C. Mansilla, P. Lovera, F. Werkoff, Can high temperature steam electrolysis function with geothermal heat? Int. J. Hydrogen Energy 32 (2007) 1174–1182.

[5] J. Sigurvinsson, C. Mansilla, B. Árnason, A. Bontemps, A. Maréchal, T.I. Sigfússon, F. Werkoff, Heat transfer problems for the production of hydrogen from geothermal energy, Energy Convers. Manage. 47 (2006) 3543–3551.

[6] M. Kanoglu, A. Ayanoğlu, A. Abusoğlu, Exergoeconomic assessment of a geothermal assisted high temperature steam electrolysis system, Energy 36 (2011) 4422–4433.

[7] M. Kanoglu, İ. Dinçer, M.A. Rosen, Geothermal energy use in hydrogen liquefaction, Int. J. Hydrogen Energy 32 (2007) 4250–4257.

[8] E. Aghaie, E. Assareh, H. Yousefi, R. Moltames, A. Fathi, K. Choubineh, Exergoeconomic optimization of a novel hydrogen generation system based on geothermal energy, Environ. Energy Econ. Res. 5 (2021) 1–15.

[9] R. Moltames, B. Azizimehr, E. Assareh, Energy and exergy efficiency improvement of a solar driven trigeneration system using particle swarm optimization algorithm, J. Sol. Energy Res. 4 (2019) 31–39.

[10] C.A. Frangopoulos, Recent developments and trends in optimization of energy systems, Energy 164 (2018) 1011–1020.

[11] A.A. Alsakati, C.A. Vaithilingam, J. Alnasseir, A. Jagadeeshwaran, Simplex search method driven design for transient stability enhancement in wind energy integrated power system using multi-band PSS4C, IEEE Access 9 (2021) 83913–83928.

[12] A. Ghadertootoonchi, A. Solaimanian, M. Davoudi, M.M. Aghtaie, Energy System Modeling and Optimization, SpringerBriefs in Energy, Springer Nature Switzerland, Cham, 2024.

[13] P. Cortés, A. Escudero-Santana, E. Barbadilla-Martin, J. Guadix, A production-inventory model to optimize the operation of distributed energy resource networks in a rolling horizon, Heliyon 10 (2024) e38112.

[14] L. Kyriakidis, R. Kansara, M.I. Roldán Serrano, Energy management of industrial energy systems via rolling horizon and hybrid optimization: a real-plant application in Germany, Energies 18 (2025) 3977.

[15] G. Thiele, T. Johanni, D. Sommer, J. Krüger, Decomposition of a cooling plant for energy efficiency optimization using OptTopo, Energies 15 (2022) 8387.

[16] A. Izadi, M. Shahafve, P. Ahmadi, Neural network genetic algorithm optimization of a transient hybrid renewable energy system with solar/wind and hydrogen storage system for zero energy buildings at various climate conditions, Energy Convers. Manage. 260 (2022) 115593.

[17] M. Wu, P. Du, M. Jiang, H.H. Goh, H. Zhu, D. Zhang, T. Wu, An integrated energy system optimization strategy based on particle swarm optimization algorithm, Energy Rep. 8 (2022) 679–691.

[18] S. Chen, S. Wang, An optimization method for an integrated energy system scheduling process based on NSGA-II improved by tent mapping chaotic algorithms, Processes 8 (2020) 426.

[19] M. Nasir, A. Sadollah, S. Mirjalili, S.A. Mansouri, M. Safaraliev, A. Rezaee Jordehi, A comprehensive review on applications of grey wolf optimizer in energy systems, Arch. Comput. Methods Eng. 32 (2025) 2279–2319.

[20] S. Stavrev, D. Ginchev, Reinforcement learning techniques in optimizing energy systems, Electronics 13 (2024) 1459.

[21] M.M. Forootan, I. Larki, R. Zahedi, A. Ahmadi, Machine learning and deep learning in energy systems: a review, Sustainability 14 (2022) 4832.

[22] M. Abdelsattar, M.A. Ismeil, M.M. Zayed, A. Abdelmoety, A. Emad-Eldeen, Assessing machine learning approaches for photovoltaic energy prediction in sustainable energy systems, IEEE Access 12 (2024) 107599–107615.

[23] R. Echrigui, M. Hamiche, Optimizing LSTM models for EUR/USD prediction in the context of reducing energy consumption: an analysis of mean squared error, mean absolute error and R-squared, in: E3S Web of Conferences, vol. 412, EDP Sciences, 2023, p. 01069.

[24] C. Wu, S.S. Wang, J. Li, Parametric study on the effects of a recuperator on the design and off-design performances for a CO2 transcritical power cycle for low temperature geothermal plants, Appl. Therm. Eng. 138 (2018) 644–658.

[25] J. Fang, M. Yang, Y. Fan, T. Luo, H. Li, T. Liu, S. Tang, K. Zhao, Thermodynamic evaluation of a combined cooling, heating, hydrogen, and power multi-generation system for full-spectrum solar energy utilization, Energy Convers. Manage. 300 (2024) 118019.